Geotechnical Engineering for the Preservation of Monuments and Historic Sites III

Edited by
Renato Lancellotta, Carlo Viggiani,
Alessandro Flora, Filomena de Silva,
and Lucia Mele

CRC Press
Taylor & Francis Group

GEOTECHNICAL ENGINEERING FOR THE PRESERVATION OF MONUMENTS AND HISTORIC SITES III

The conservation of monuments and historic sites is one of the most challenging problems facing modern civilization. It involves, in inextricable patterns, factors belonging to different fields (cultural, humanistic, social, technical, economical, administrative) and the requirements of safety and use appear to be (or often are) in conflict with the respect of the integrity of the monuments. The complexity of the subject is such that a shared frame of reference is still lacking among art historians, architects, architectural and geotechnical engineers. And while there are exemplary cases of an integral approach to each building element with its static and architectural function, as a material witness to the culture and construction techniques of the original historical period, there are still examples of uncritical reliance on modern technology leading to the substitution from earlier structures to new ones, preserving only the iconic look of the original monument. Geotechnical Engineering for the Preservation of Monuments and Historic Sites III collects the contributions to the eponymous 3rd International ISSMGE TC301 Symposium (Naples, Italy, 22–24 June 2022). The papers cover a wide range of topics, which include:

- Principles of conservation, maintenance strategies, case histories
- The knowledge: investigation, monitoring and performance
- Seismic risk, site effects, soil structure interaction
- Effects of urban development and tunnelling on built heritage
- Preservation of diffuse heritage: soil instability, subsidence, environmental damages

The present volume aims at geotechnical engineers and academics involved in the preservation of monuments and historic sites worldwide.

PROCEEDINGS OF THE THIRD INTERNATIONAL ISSMGE TC301 SYMPOSIUM, NAPOLI, ITALY, 22–24 JUNE 2022

Geotechnical Engineering for the Preservation of Monuments and Historic Sites III

Edited by

Renato Lancellotta
Department of Structural, Geotechnical and Building Engineering
Politecnico di Torino, Turin, Italy

Carlo Viggiani, Alessandro Flora, Filomena de Silva & Lucia Mele
Department of Civil, Architectural and Environmental Engineering
University of Naples Federico II, Naples, Italy

CRC Press
Taylor & Francis Group
Boca Raton London New York Leiden

CRC Press is an imprint of the
Taylor & Francis Group, an **informa** business
A BALKEMA BOOK

CRC Press/Balkema is an imprint of the Taylor & Francis Group, an informa business

Typeset in Times New Roman by MPS Limited, Chennai, India

Library of Congress Cataloging-in-Publication Data

A catalog record has been requested for this book

First published 2022

Published by: CRC Press/Balkema
Schipholweg 107C, 2316 XC Leiden, The Netherlands
e-mail: enquiries@taylorandfrancis.com
www.routledge.com – www.taylorandfrancis.com

ISBN: 978-1-032-31262-0 (Hbk)
ISBN: 978-1-032-31265-1 (Pbk)
ISBN: 978-1-003-30886-7 (ebk)
DOI: 10.1201/9781003308867

An influence of the water supply in improved soil against liquefaction 792
N. Özbakan & B. Evirgen

Site characterization and preliminary ground response analysis for the monumental Complex of SS. Annunziata in Sulmona, Italy 800
C. Madiai, G. Ciardi, M. Manuel, F. Galadini & S. Amoroso

A simplified method for the estimation of earthquake-induced pore pressures 812
G. Boccieri, D. Gaudio & R. Conti

Evaluation of DSSI for the preservation of the Catania University Central Palace 823
G. Abate, S. Corsico, A. Fiamingo, S. Grasso & M.R. Massimino

Vulnerability assessment of historical cities including SSI and site-effects 836
C. Amendola & D. Pitilakis

Effects of local soil conditions on the seismic response of the historical area in San Giuliano di Puglia (Italy) 847
T. Fierro, M. Castiglia, F. Santucci de Magistris & M.G. Durante

Simulation of damage observed on buildings in aggregate after the 2016–2017 Central Italy earthquake accounting for site effects and soil-structure interaction 859
A. Brunelli, G.A. Alleanza, S. Cattari, F. de Silva & A. d'Onofrio

A large-scale evaluation of the seismic demand for historic towers laying on soft soil 871
F. de Silva & F. Silvestri

Dynamic impedance functions for neighbouring shallow footings 883
E. Zeolla, S. Sica & F. de Silva

A Geotechnical Study for the Historical Heritage Preservation of the City of Noto (Italy) 893
A. Cavallaro

Soil contribution on the structural identification of a historical masonry bell-tower: Simplified vs advanced numerical models 904
A. De Angelis, A. Ambrosino, S. Sica & P.B. Lourenco

The geotechnical seismic isolation of historical buildings through polyurethane injections: A numerical study 917
M.P.A. Gatto & L. Montrasio

Conservation of ancient Zrug church after landslide 930
I. Strelbitsky

SESSION 4: Effects of urban development and tunnelling on the built heritage

Municipio Station Metro Line 6 in Naples: A case of urban tunnelling adopting ground freezing and grouting techniques to underpass archaeological findings 937
G. Russo, F. Cavuoto, A. Corbo & V. Manassero

The design of Venezia station of Rome Line C underground 951
E. Romani, M. D'Angelo, L. Sidera & A. Sciotti

Improvement of foundation soil behavior for Gründerzeit buildings in Austria using polyurethane resin injections 964
A. Dominijanni, M. Gabassi, F.F. Kopf, A. Minardi & A. Pasquetto

Geotechnical Engineering for the Preservation of Monuments and Historic Sites III – Lancellotta, Viggiani, Flora, de Silva & Mele (Eds)

A simplified method for the estimation of earthquake-induced pore pressures

G. Boccieri
Università di Roma Niccolò Cusano, Rome, Italy

D. Gaudio
Sapienza Università di Roma, Rome, Italy

R. Conti
Università di Roma Niccolò Cusano, Rome, Italy

ABSTRACT: A reliable assessment of liquefaction hazard is crucial for reducing the seismic risk of existing structures, especially for historical heritage. Common practice would need earthquake-induced pore pressures to be evaluated through simple methods, such as *uncoupled* approaches. *Uncoupled* approaches based on undrained cyclic laboratory tests originate from Seed et al. (1975), where seismic-induced rate of excess pore pressure build-up under fully-undrained conditions was added to the one-dimensional consolidation equation by Terzaghi. Despite its simplicity, this approach allows to consider the key features of liquefaction, as the influence of partially-drained conditions and pore pressures dissipation. In this paper, a simplified method based on Seed et al. (1975) is presented, aimed at estimating earthquake-induced pore water pressures. The governing equation is solved using the Finite Difference Method, by taking into account the dependence of soil stiffness on current mean effective stress. Different strategies for modelling the source term are presented and discussed.

1 INTRODUCTION

Under medium-to-high intensity earthquakes, excess pore water pressures may develop in saturated sandy soil layers exhibiting an undrained or a partially drained response, thus reducing the effective stress state acting into the soil, and, consequently, its shear stiffness and strength. This effect may result in catastrophic consequences for structures resting on liquefied soils, as recognised in post-earthquake surveys conducted worldwide after strong-motion earthquakes, such as the well-known ones occurred in Niigata (1964), (Kramer 1996), Kobe (1995), Shibata et al. (1996), Christchurch (2010) and (Cubrinovski et al. 2011). More recently, the Emilia earthquake (2012) (Mucciarelli & Liberatore 2014) caused severe damages to the historical heritage, such as façades and bell towers of churches (Sorrentino et al. 2013a), medieval fortresses and vernacular buildings (Sorrentino et al. 2013b). Therefore, there is a strong need of developing procedures to obtain a reliable estimate of the liquefaction hazard and, consequently, of the excess pore water pressures accumulated in saturated sandy soil deposits.

Two different approaches are available for evaluating the excess pore water pressures induced by earthquakes (Chiaradonna et al. 2018), namely the *decoupled* approach and the *coupled* approach. The *decoupled* approach is typically adopted for simplified liquefaction analyses and therefore followed by national codes: in this case, semi-empirical equations based on the results of ground response analyses performed neglecting the bi-phasic nature of soils (i.e. total stress approach) are used. In spite of its simplicity, this approach requires some arbitrary tasks, such as the definition of an equivalent cyclic loading for the irregular seismic-induced shear stresses, in terms of induced excess pore water pressures (Seed et al. 1975). Conversely, the *coupled* approach relies on rigorous Finite Element or Finite Difference nonlinear (effective stresses) dynamic analyses. In this case, less (still different from zero though) arbitrary assumptions must be introduced, but more onerous and time-consuming analyses must be carried out.

 DOI 10.1201/9781003308867-62

Following a *decoupled* approach, this paper presents a simplified method for the evaluation of earthquake-induced pore pressures in liquefiable soils. The method is based on the seminal work by Seed et al. (1975), who modified the well-known 1D consolidation equation (Terzaghi 1923) by adding a source term due to earthquake shaking, representing the rate of excess pore water pressure build-up under fully-undrained conditions. The procedure is implemented in a home-made Matlab program through the Finite Difference Method. The simple constitutive approach recently proposed by Conti et al. (2020) is adopted to perform the preliminary 1D nonlinear ground response analysis, necessary for a proper estimate of the shear stress time histories acting into the soil and therefore of the number of cycles to liquefaction. The good estimate of excess pore water pressures obtained via the proposed simplified method is demonstrated through the comparison with a case study from the literature where a *coupled* approach was followed (Chiaradonna et al. 2019).

Overall, the proposed method aims at providing a simplified but physically-sound solution of the problem, which captures the main physical aspects of the liquefaction phenomenon while keeping a good balance in between accuracy and ease of use.

2 IMPLEMENTATION OF THE SIMPLIFIED METHOD

Seed et al. (1975) proposed a *decoupled* approach to evaluate the development and redistribution of seismic-induced excess pore water pressures, u, in a horizontally-stratified soil deposit, based on the results of cyclic undrained tests. The key idea was adding to the one-dimensional consolidation equation by Terzaghi (Terzaghi 1923) a source term due to earthquake shaking:

$$\frac{\partial u}{\partial t} = c_{\mathrm{v}} \cdot \frac{\partial^2 u}{\partial z^2} + \frac{\partial u_{\mathrm{g}}}{\partial t} \tag{1}$$

where the first term on the right side is the classical dissipative term, proportional to the consolidation coefficient c_v, and the second one is the above-mentioned source term, representing the rate of excess pore water pressure build-up under fully-undrained conditions. Despite its very simplicity, Equation (1) provides an immediate picture of the pore pressure generation phenomenon under partially drained conditions. Indeed, if the first term on the right side of the equation is relatively small, excess pore pressures $\partial u/\partial t$ would be similar to those developed in undrained conditions, $\partial u_g/\partial t$. Conversely, if the two terms on the right side match each other, the soil response would result perfectly drained and all the earthquake-induced pore pressures would be instantaneously dissipated by the soil layer. Finally, when the second term is relatively small or null, then soil behaviour is ruled by 1D consolidation. This is the case, for example, of the post-earthquake stage, where possible excess pore water pressures are gradually dissipated within the soil deposit.

In the light of a *decoupled* approach, the source term must be related to the driving shear stresses, $\tau(t)$, induced by the seismic waves into the soil, and the latter can be computed by means of simple 1D Linear Equivalent or Nonlinear site response analyses. To this end, the seismic-induced time history of shear stress is conventionally replaced with a cyclic loading characterised by a constant amplitude, τ_{eq} (typically assumed as the 65% of the maximum shear stress τ_{max}), and by an equivalent number of cycles, N_{eq}, uniformly distributed over the cyclic loading duration, T_d. Following this procedure, the source term can be rewritten as:

$$\frac{\partial u_{\mathrm{g}}}{\partial t} = \frac{\partial u_{\mathrm{g}}}{\partial N} + \frac{\partial N}{\partial t} = \frac{\sigma'_{\mathrm{v0}}}{N_{\mathrm{L}}} \cdot \frac{\partial r_{\mathrm{u}}}{\partial r_{\mathrm{N}}} \cdot \frac{N_{\mathrm{eq}}}{T_{\mathrm{d}}} \tag{2}$$

where $r_{\mathrm{u}} = u_{\mathrm{g}}/\sigma'_{\mathrm{v0}}$ is the pore pressure ratio; $r_{\mathrm{N}} = N/N_{\mathrm{L}}$ is the cyclic ratio; N is the n-th cycle of loading; and N_{L} is the number of cycles needed to trigger liquefaction (i.e. $u_{\mathrm{g}} = \sigma'_{\mathrm{v0}}$ and therefore $r_{\mathrm{u}} = 1$). Under these assumptions, Seed & Booker (1977) expressed r_{u} as a function of r_{N} through an analytical expression which fitted the results of cyclic laboratory tests carried out in undrained conditions, as follows:

$$r_{\mathrm{u}} = \frac{2}{\pi} \cdot \sin^{-1}\left(r_{\mathrm{N}}^{\frac{1}{2\alpha}}\right) \tag{3}$$

where α is a function of soil current state and test conditions.

If the number of cycles required to trigger liquefaction, N_L, is known, together with the duration T_d and the equivalent number of cycles N_{eq}, then the rate of excess pore water pressures developing under fully-undrained conditions, $\partial u_g/\partial t$, can be computed through Equation (2).

The recalled model by Seed et al. (1975) was implemented in Matlab v.9.10.0 (R2021a) (MATLAB 2021) through the Finite Difference Method (FDM) for the specific case of a double-layered soil deposit. The following additional assumptions were introduced:

(i.) the deepest stratum is susceptible to liquefaction, being ruled by Equation (1);
(ii.) in the shallowest layer, redistribution of pore water pressure takes place only, which is governed by the classical equation by Terzaghi (i.e. $\partial u_g/\partial t = 0$);
(iii.) two conditions were imposed at the interface between the two layers, namely the water flow continuity and the pore water pressure equilibrium;
(iv.) free drainage is allowed at the groundwater level only (i.e. impervious boundary at the bottom of the soil column);
(v.) the shear stiffness modulus, G, is a function of the mean effective stress p'.

The last assumption allows taking into account the effect of the progressive reduction (or recovery) of soil shear stiffness on the generation and redistribution of pore water pressures during both the strong motion and post-earthquake stages of the analysis.

In the following of this section, evaluation of N_L, N_{eq}, T_d and $G(p')$ is illustrated.

2.1 *Number of cycles to liquefaction* N_L

The number of uniform cycles needed to produce liquefaction, N_L, was obtained from experimental cyclic resistance curves $CSR - N_L$. The cyclic stress ratio $CSR = \tau_{eq}/\sigma'_{v0}$ can be evaluated from the maximum shear stresses τ_{max} generated by the seismic event, which can be derived through either a seismic response analysis or a simplified procedure. It is worth noting that, since uncertainties arising in the simplified procedure increase with depth, the latter should be applied only for depths less than about 20 m, while liquefaction evaluations at greater depths should be based on seismic response analysis (Idriss & Boulanger 2006).

The relationship between CSR and N_L, within the range of cycles of interest for earthquake engineering, can be approximated through a power function as (Idriss & Boulanger 2008):

$$CSR = \beta \cdot N_L^{-\eta} \tag{4}$$

where β and η are coefficients mainly depending on the relative density D_R, defining the intercept and the slope of the curve in a semi-logarithmic plane, and can be determined from experimental data.

2.2 *Properties of the equivalent cyclic loading,* N_{eq} *and* T_d

The irregular seismic-induced time history of shear stress is replaced by an equivalent cyclic loading, which, in principle, should produce the same increase of excess pore water pressures in the soil sample under a fully undrained condition.

The conversion procedure is based on the hypothesis of linear damage accumulation proposed by Miner (1945) for the calculation of fatigue damage in aluminium (Biondi et al. 2012; Hancock & Bommer 2005). The additional assumption of considering the horizontal acceleration rather than the shear stress time history was made in this study, thanks to their direct proportionality (Biondi et al. 2012). Considering the curves $CSR - N_L$ as the loci of same damage level (i.e. initial liquefaction of soil sample), the number of equivalent cycles N_{eq} of a cyclic loading with amplitude $a_{eq} = 0.65\ a_{max}$, where a_{max} is the maximum value of the acceleration signal, can be computed as:

$$N_{eq} = \sum_i N_i \cdot \left(\frac{a_{eq}}{a_i}\right)^{-1/\eta} \tag{5}$$

where N_i is the number of cycles with amplitude a_i of the initial signal and η is the same coefficient as in Equation (4).

A method for calculating the number of cycles of the accelerometric signal was therefore necessary. To this end, the peak-counting method was adopted, where the number of largest peaks between adjacent zero-crossing is explicitly counted (Hancock & Bommer 2005). Every peak encountered in between two adjacent zeros identifies a hemicycle ($N_i = 0.5$ in Eq. (5)).

The equivalent number of cycles N_{eq} can be considered either variable with depth, when a seismic site response analysis providing acceleration time histories at the different depths is performed, or equal to a constant value within the soil column. In the latter case, deriving N_{eq} directly from the input signal at the bedrock is not recommended, since the applied acceleration is likely to be filtered by the overlying deformable soil layers. Therefore, it would be more appropriate to consider the signal either at the free-field ground surface or at an adequate, intermediate depth of the liquefiable layer.

The cyclic loading duration T_d was taken equal to the strong motion duration of the acceleration time history computed either at the soil surface or within the liquefiable soil layer. Specifically, T_d was defined following Trifunac and Brady (1975), as the range spanned by time intervals when Arias intensity reaches its 5% and 95% of its final value. Hereby it is worth mentioning that the influence of soil deformability on T_d is much less pronounced than for N_{eq}.

2.3 *Soil stiffness*

Empirical relationships typically adopted for the small-strain shear modulus G_0 of sands assume the following functional form (Viggiani & Atkinson 1995; Wichtmann & Triantafyllidis 2009):

$$G_0 = F(e) \cdot (p'_0)^{0.5} \tag{6}$$

where $F(e)$ is a function of void ratio e and grain size distribution, while p'_0 is the initial mean effective stress. In this study, the same relationship was used to compute the current value of the soil shear modulus at any time instant during the seismic excitation. To this end, the initial stress state was replaced by the current mean effective stress, p', as variations of the effective stress state can be remarkable due to the possible high development of excess pore water pressure during shaking. This aspect is crucial for an accurate simulation of both the generative and dissipative terms (Adamidis & Madabhushi 2016) and allowed to take into account the dependency of the oedometric modulus, E_{oed},and of the 1D consolidation coefficient, c_v, on the current effective stress, defined as:

$$E_{oed} = \frac{2G(1-\nu)}{(1-2\nu)} \tag{7}$$

$$c_v = \frac{k \cdot E_{oed}}{\gamma w} \tag{8}$$

where G is the current shear modulus, depending on the actual mean effective stress, ν is the Poisson ratio, k is the (vertical) hydraulic conductivity, and $\gamma_w = 9.81$ kN/m^3 is the unit weight of water.

3 1D NONLINEAR SITE RESPONSE ANALYSIS

Liquefaction is typically triggered by medium-to-high intensity earthquakes, which cause significant accelerations within the soil deposit. For this reason, the profile of maximum shear stress, $\tau_{max}(z)$, should be derived by means of Nonlinear seismic site response analyses rather than Linear Equivalent ones. This way, the amplitude of the equivalent cyclic loading, τ_{eq}, and the number of cycles to liquefaction, N_L, are computed properly.

In this work, a 1D Nonlinear site response analysis was used to compute $\tau_{max}(z)$. To this end, the 1D dynamic equilibrium equation was solved through the Finite Difference Method, implemented

in a home-made Matlab program. The nonlinear soil model recently proposed by Conti et al. (2020) was used, including both nonlinearity and shear strength as constitutive ingredients. The model combines the hyperbolic functional form introduced by Hardin and Drnevich (1972) for the backbone curve with the unloading-reloading rule suggested by Phillips & Hashash (2009). The main novel contribution of the new approach was linking the nonlinear soil behaviour to its small strain stiffness and shear strength through functions of effective stresses. As a result, prediction of 1D cyclic behaviour of soils was improved despite the reduction of soil parameters (only six), compared to previous models (Phillips & Hashash 2009). Four out of the six parameters (a, b, c and d) depend solely on the nature of soil and can be easily calibrated against one single cyclic laboratory test, while the two remaining ones (τ_{lim} and G_0) depend also on the effective stress, and can be obtained from either standard penetration and seismic field tests or laboratory tests.

The steps followed to implement the adopted constitutive soil model within the 1D nonlinear code are summarised below:

i. determine the small-strain shear modulus and shear strength profiles, $G_0(z)$ and $\tau_{lim}(z)$, both depending on the effective stress state;
ii. for each material within the soil column, calibrate parameters a, b, c and d against experimental shear modulus degradation and damping curves, $G(\gamma)/G_0$ and $D(\gamma)$,where γ is the shear strain. Here it is worth noting that the experimental (or empirical) curves should refer to a single value of p', as the dependency on the effective stress state is already enclosed in the shear stiffness and strength profiles from previous point.;
iii. divide the soil column in layers with constant values of G_0 to input the dependence of the small-strain shear modulus on the depth (via the effective stress state);
iv. assign a, b, c, d, G_0 and τ_{lim} as constitutive parameters and make use of the constitutive equations proposed Conti et al (2020).

4 VALIDATION ON A CASE STUDY

This section aims at demonstrating the capability of the simplified method outlined in this paper of predicting the excess pore water pressures induced by the earthquake within the soil deposit and possibly leading to full liquefaction. Specifically, a comparison with the case study recently presented by Chiaradonna et al. (2019) is made, where the seismic performance of a levee of an irrigation channel, which was severely damaged during the 2012 Emilia earthquake, was considered. The study was carried out considering a reference soil column which was subjected to a seismic shaking in a 1D *coupled* dynamic analysis performed in terms of effective stresses via the code SCOSSA (Tropeano et al. 2016), where the build-up of excess pore water pressures is computed based on the definition of a "damage parameter" (Chiaradonna et al. 2018). Conversely, a two-steps *uncoupled* procedure was followed in this work. First, a 1D nonlinear ground response analysis was performed through the one-dimensional home-made computer program presented in Conti et al. (2020) to obtain the equivalent cyclic loading and, therefore, the number of cycles to liquefaction, N_L (§ 3). Second, the seismic-induced excess pore water pressures were computed through the method by Seed et al. (1975) (§ 2).

In the following sections, a comparison with the results obtained by Chiaradonna et al. (2019) is presented. For the sake of clarity, the results of the 1D ground response analysis and the evaluation of seismic-induced excess pore water pressures will be discussed separately.

4.1 *1D nonlinear seismic response analysis*

The nonlinear seismic site response analysis was carried out for a 115 m-deep layered soil column. The dyke and its foundation soil consist of a silty sand layer overlying a thick deposit of alluvial sands, alternated with layers of clay. The saturated silty sand and the shallowest sand layers are potentially liquefiable.

Figure 1 shows the soil stratigraphy along with the small-strain shear wave velocity, V_{S0}, profiles adopted in this study and in Chiaradonna et al. (2019), while Figure 2 displays the shear modulus

degradation and damping curves considered by Chiaradonna et al. (2019), together with those utilized in this study.

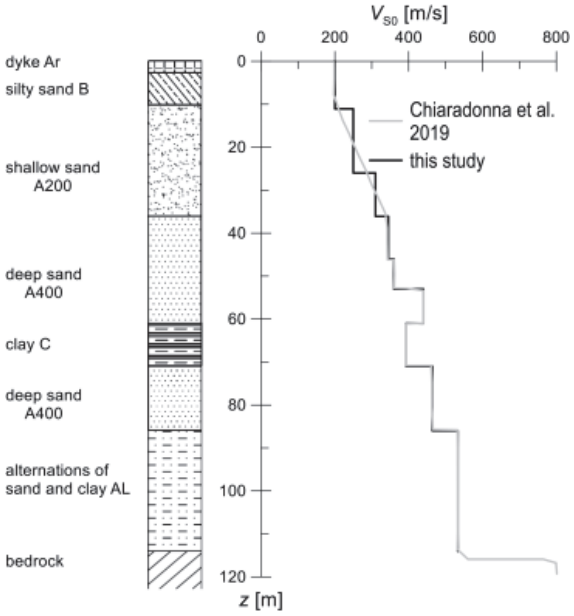

Figure 1. Soil stratigraphy and profile of the small-strain shear wave velocity.

The six parameters required to define the constitutive soil model were calibrated against the strength parameters reported in Chiaradonna et al. (2019) and the laboratory data published by Tonni et al. (2015). These are listed in Table 1, where: z_{top} and z_{bottom} are the depths of the top and the bottom of each layer, measured starting from the ground surface, and $\Delta z = z_{top} - z_{bottom}$ is the corresponding thickness; a and b are the parameters defining the shear modulus degradation curves, while c and d define the damping curves; φ' is the soil friction angle; σ'_0 is either the vertical or the mean effective stress, depending on relevant laboratory test performed to obtain the strength and stiffness parameters (dual-specimen direct simple shear, DSDSS, or resonant column, RC); $V_{S0} = \sqrt{(G_0/\rho)}$ is the small-strain shear wave velocity; ρ is the mass density of soils; ν is the Poisson ratio and k is the hydraulic conductivity.

Table 1. Model parameters adopted in this study.

Soil	z_{top} m	z_{bottom} m	Δz m	a –	b –	c –	d –	φ' °	σ'_0 kPa	V_{S0} m/s	ν –	k m/s
Dyke	0	2.5	2.5	0.73	0.10	0.70	1.73	33	100	145	0.306	$1 \cdot 10^{-6}$
Silty sand	2.5	10.0	7.5	0.73	0.10	0.70	1.73	33	100	145	0.306	$1 \cdot 10^{-6}$
Sand A200	10.0	35.0	25.0	1.09	0.10	0.63	2.31	38	200	175	0.286	$3 \cdot 10^{-5}$
Sand A400	35.0	61.0	26.0	1.92	0.10	0.55	1.02	38	400	215	0.286	$3 \cdot 10^{-5}$
Clay	61.0	71.0	10.0	0.10	10.0	0.84	1.84	25.5	100	160	0.371	$1 \cdot 10^{-8}$
Sand A400	71.0	86.0	15.0	1.92	0.10	0.55	1.02	38	400	215	0.286	$3 \cdot 10^{-5}$
Alter. AL	86.0	115.0	29.0	1.16	0.10	0.47	1.31	33	400	215	–	–

The input motion adopted in the seismic site response analysis is plotted in Figure 3, in terms of horizontal acceleration time history (a) and Fourier amplitude spectrum (b). The original signal was low-pass filtered at a frequency f_{max} = 10 Hz, through an 8th-order lowpass Butterworth filter, and then brought back to the initial peak ground acceleration *PGA*, equal to 0.344 *g*. The input signal was applied as an outcrop motion.

The results obtained from the nonlinear seismic site response analysis are presented in Figure 4 in terms of a_{max}, τ_{max} and γ_{max}. The maximum shear stresses τ_{max} obtained in this study through the

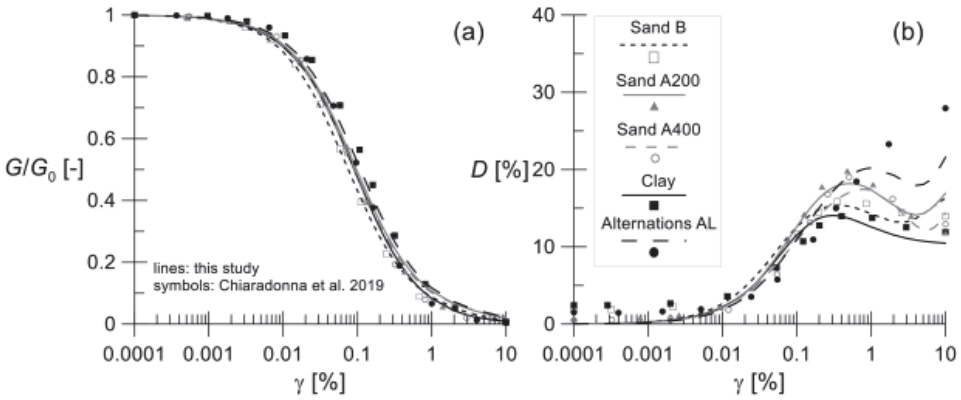

Figure 2. (a) Shear modulus degradation curves and (b) damping curves adopted in this study and in Chiaradonna et al. (2019).

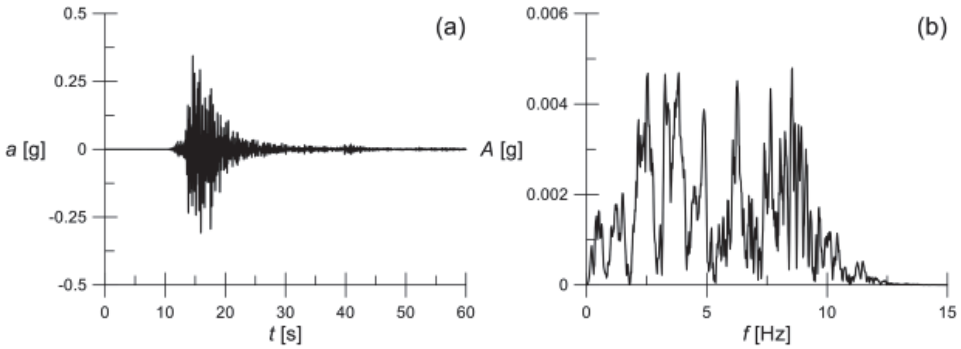

Figure 3. (a) Horizontal acceleration time history and (b) Fourier amplitude spectrum of the input motion adopted in the seismic site response analysis.

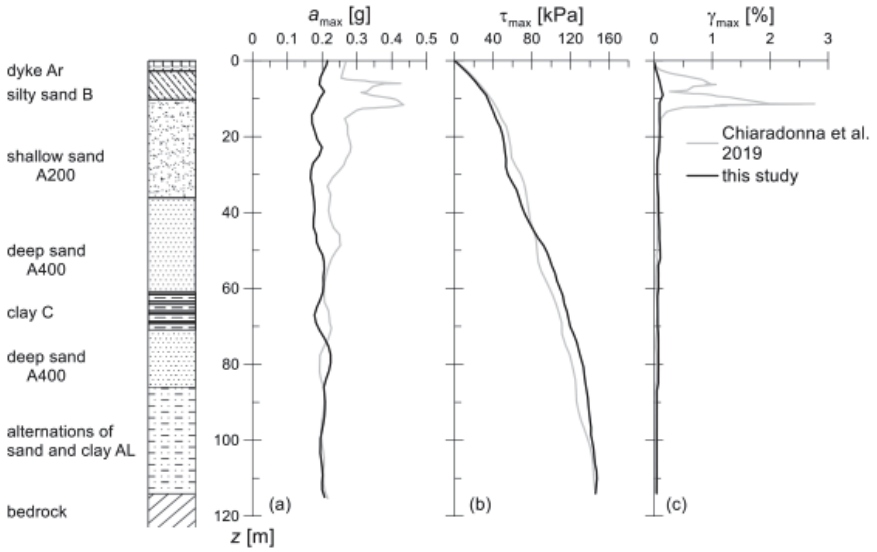

Figure 4. Profiles of the (a) peak acceleration, (b) maximum shear stress and (c) maximum shear strain.

decoupled approach are quite in a good agreement with those provided by Chiaradonna et al. (2019). This result clearly stems from the fact that, even following a more rigorous *coupled* approach, the maximum shear stresses within a liquefiable soil layer are reached before triggering liquefaction, thus they are not affected by the subsequent liquefaction-related stiffness degradation and damping increase. This aspect is evident by inspection of Figure 5, showing (a) the time history of shear stresses and excess pore pressure ratio, r_u, computed at z = 2.2 m by Chiaradonna et al. (2019) and

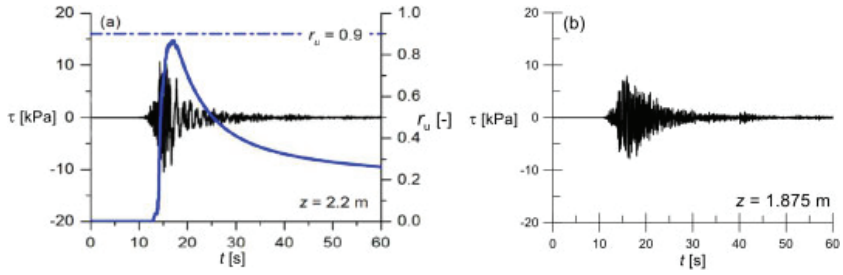

Figure 5. (a) Shear stress time history over the liquefied layer in the case study (after Chiaradonna et al. 2019) and (b) in this study through the proposed *decoupled* approach.

(b) the shear stress computed at $z = 1.875$ m in this work. On one hand, the two approaches provide comparable results in terms of maximum shear stresses. On the other hand, the decoupled approach cannot reproduce the significant filtering of shear stress occurring once the full liquefaction condition is triggered within the shallow sand layers. Conversely, the main difference between the two approaches lies in the maximum shear strain developed close to the ground surface. This is due to the inherent inability of the *decoupled* approach of estimating the high deformations produced by the liquefaction phenomena.

4.2 *Evaluation of seismic-induced excess pore water pressures*

A proper evaluation of the seismic-induced excess pore water pressures requires a preliminary calibration of the parameters defining the $r_u - r_N$ (Eq. (3)) and $CSR - N_L$ (Eq. (4)) relationships. Experimental data for the sand layers (A200 and A400) and the silty sand (B) were provided in Chiaradonna et al. (2019). Considering only sand data, the best-fitting values of α for the $r_u - r_N$ curve (Figure 6a), β and η, for the liquefaction resistance curve (Figure 6b), are equal to 0.890, 0.345 and 0.285, respectively. From the comparison between the liquefaction resistance curve used in the present work and in the case study, it turns out that the two curves are in good agreement, at least for the range of *CSR* and N_L values of interest, as obtained from the site response analysis (grey-shaded area in Figure 6b). Furthermore, the $r_u - r_N$ curve proposed by Seed et al. (1975) was scaled by a factor of 0.9 to be in agreement with Chiaradonna et al. (2019), who set the threshold for initial liquefaction at $r_u = 0.9$ (Figure 6a).

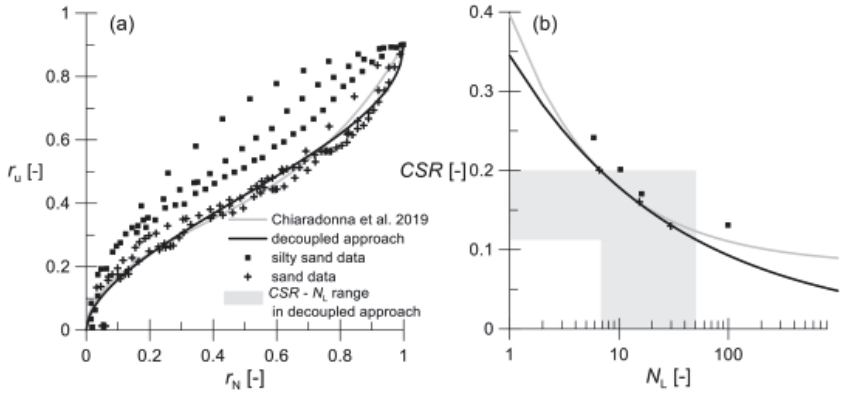

Figure 6. (a) Pore water pressure relationship (Eq. (3)) and (b) cyclic resistance curves (Eq. (4)) adopted in the present study and in Chiaradonna et al. (2019).

The geometry of the multi-layered soil deposit (Figure 1) was simplified into a double-layered soil column for evaluating the seismic-induced excess pore water pressures through Eqs. (1)–(2). The soil column was divided into a superficial 2-m-thick non-liquefiable layer, corresponding to the previous dyke (Ar) stratum, underlain by a 58-m-thick potentially liquefiable layer, this

representing all the sandy soils (B, A200, and A400) resting on the clay layer (C). The clay layer was modelled as an impervious boundary, consistently with Chiaradonna et al. (2019) who showed null excess pore water pressures ($r_u = 0$) below depth $z = 60$ m. The groundwater level was located at depth $z_w = 2$ m and the initial pore water pressure regime was hydrostatic.

In order to assess the influence of the hypothesis made on the equivalent number of cycles, N_{eq}, two different analyses were performed, assuming that N_{eq} either varies with depth (Figure 7), or is constant (Figure 8). Conversely, in both cases the duration of the equivalent cyclic loading, T_d, was considered constant with depth.

In the first analysis, the duration of the equivalent cyclic loading, $T_d = 10.48$ s, was evaluated from the horizontal acceleration time history computed at the ground surface ($z = 0$) in the 1D nonlinear seismic response analysis (Figure 7b). The two vertical black lines in Figure 7d indicate the corresponding time interval of the strong motion stage. By inspection of Figure 7b, it can be observed that the T_d value computed at ground surface is very close to the average valued computed along the entire soil column. In this analysis, liquefaction was triggered in between depths $z = 2 – 21$ m ($r_{u\ max} = 0.9$, Figure 7c), corresponding to the depth range where $N_{eq} > N_L$ (Figure 7a): the simplified analysis therefore predicts liquefaction occurring within the silty sand (B) and the most superficial part of the shallow sand (A200). This result is in agreement with Chiaradonna et al. (2019), whose 1D *coupled* dynamic analysis estimated liquefaction happening in a thinner part of deposit though ($z = 3 – 12$ m). From the contours of the pore pressure ratio, r_u, it turns out that no excess pore water pressure is computed before the strong-motion phase started, as expected when using the simplified model by Seed et al. (1975). Then, liquefaction is rapidly triggered in the shallowest part of the soil column while the equivalent cyclic loading is applied. Finally, dissipation of seismic-induced excess pore water pressures takes place over the whole soil column, except for what obtained around the mid-height ($z \approx 30$ m), where pore water pressures slightly increase. It is worth noting that this result shows the capability of the simplified method of reproducing even possible post-earthquake liquefaction.

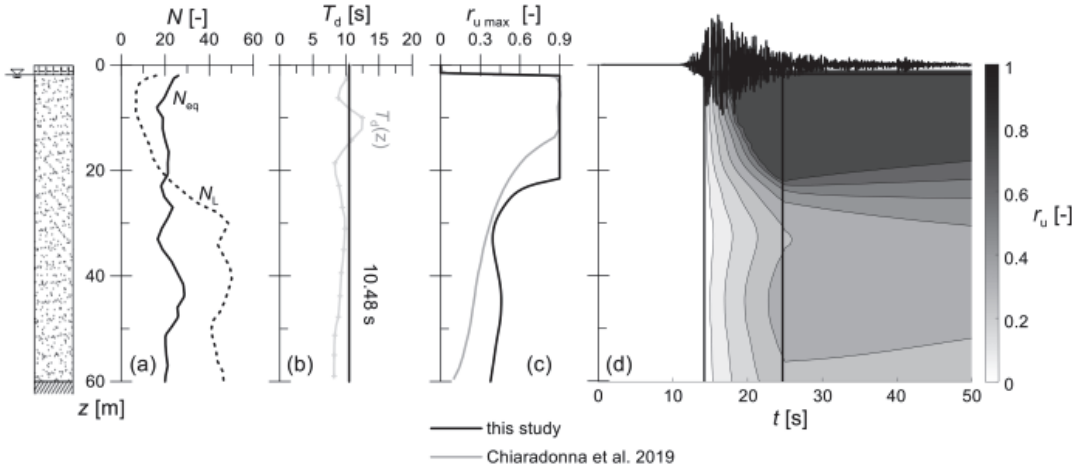

Figure 7. Main results from the analysis performed assuming an equivalent number of cycles varying with depth: profiles of (a) equivalent and limit (i.e. to liquefaction) number of cycles, (b) significant duration, (c) maximum pore pressure ratio with depth, together with (d) contours of the pore pressure ratio.

The results obtained in the second analysis, where N_{eq} is constant with depth, are given in Figure 8. This time, both N_{eq} and T_d were obtained from the acceleration time history computed at the mid-height of the liquefiable layer ($z \approx 30$ m), being equal to 18.42 and 9.85 s, respectively. Selection of time trace at the mid-height comes after observing that the corresponding values of both N_{eq} and T_d are close to the relevant average values computed along the soil column ($N_{eq,av} = 21.4$ and $T_{d,av} = 9.40$ s). Figure 8 shows that the adopted assumption on the equivalent number of cycles does not affect the results noticeably. Therefore, this further simplifying assumption may be deemed adequate for preliminary evaluation of the seismic-induced excess pore water pressures.

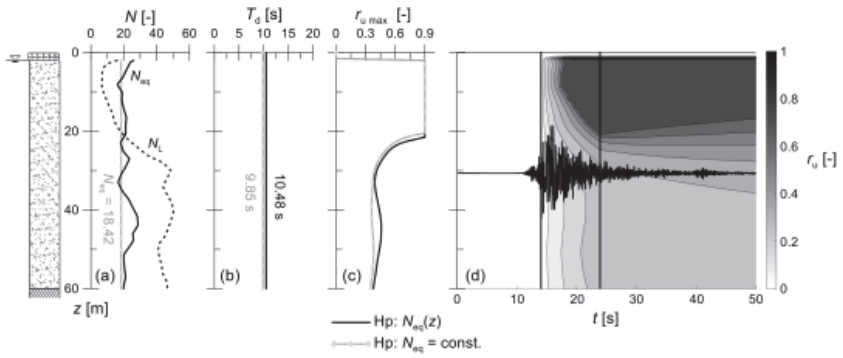

Figure 8. Main results from the analysis performed assuming an equivalent number of cycles constant with depth: profiles of (a) equivalent and limit (i.e. to liquefaction) number of cycles, (b) significant duration, (c) maximum pore pressure ratio with depth, together with (d) contours of the pore pressure ratio.

5 SYNOPSYS AND CONCLUSIONS

A reliable assessment of liquefaction hazard is crucial for reducing the seismic risk of existing structures, with reference also to monuments and historic sites, which may result more vulnerable to soil liquefaction. In this context, the development of a ready-to-use but still physically-sound simplified method for evaluating the seismic-induced excess pore water pressures accumulated into liquefiable soils is deemed necessary, as this assessment still relies on onerous and time-consuming *coupled* nonlinear dynamic analyses.

This paper presented a simplified method for the evaluation of earthquake-induced pore pressures, which was developed starting from the seminal work by Seed et al. (1975). In the method, the number of cycles needed to trigger soil liquefaction and the consequent development of excess pore water pressures can be easily calibrated against routine cyclic laboratory tests. Moreover, an equivalent cyclic loading must be defined, through its amplitude τ_{eq}, its equivalent number of cycles N_{eq}, and its duration T_d.

The procedure was implemented in a home-made Matlab program through the Finite Difference Method, where two key features were introduced, such as the dependence of soil stiffness on the current effective stress state and the variation of the equivalent number of cycles with depth.

An accurate computation of the maximum shear stresses imposed to the foundation soils is of the utmost importance for a reliable estimate of the number of cycles to liquefaction N_L. In the presence of medium-to-high intensity earthquakes, such as those usually causing liquefaction, the usual free-field ground response analysis performed through the Linear Equivalent Method would provide inaccurate results and therefore a nonlinear analysis is needed. Moreover, in order to account for both nonlinearity and strength into the constitutive soil equations, the simple approach recently proposed by Conti et al. (2020) has been adopted, being defined by few parameters which can be easily calibrated. Although not being able of considering the bi-phasic nature of soils, this approach turned out to provide peak shear stresses in a very good agreement with those computed through more rigorous 1D *coupled* nonlinear dynamic analyses. This result, which was attributed to the fact that maximum shear stresses within a liquefiable soil layer must occur well before the attainment of liquefaction, is of great relevance when following a *decoupled* approach to estimate earthquake-induced pore pressures build-up. Clearly, simple 1D nonlinear analyses cannot reproduce the development of shear strains and filtering effects induced by liquefaction.

After computing the number of cycles to liquefaction N_L through the 1D nonlinear analysis, the simplified method by Seed et al. (1975) was used to estimate the seismic-induced excess pore water pressures into the liquefiable soils for the reference case study. Again, the comparison with results available in the literature turned out to be more than satisfactory in terms of soil thickness reaching liquefaction, bearing in mind the simplicity of the proposed method. Moreover, the influence of the assumption on the equivalent number of cycles N_{eq}, whether variable with depth or constant, did not affect the results noticeably.

REFERENCES

Adamidis, O. & Madabhushi, G.S.P. 2016. Post-liquefaction reconsolidation of sand. *Proceedings of the Royal Society A: Mathematical, Physical and Engineering Sciences*, 472(2186): 20150745.

Biondi, G., Cascone, E. & Di Filippo, G. 2012. Affidabilità di alcune correlazioni empiriche per la stima del numero di cicli di carico equivalente. *Rivista Italiana di Geotecnica* 46(2): 9–39. [in italian]

Chiaradonna, A., Tropeano, G., d'Onofrio, A. & Silvestri, F. 2018. Development of a simplified model for pore water pressure build-up induced by cyclic loading. *Bulletin of Earthquake Engineering* 16(9): 3627–3652.

Chiaradonna, A., Tropeano, G., d'Onofrio, A. & Silvestri, F. 2019. Interpreting the deformation phenomena of a levee damaged during the 2012 Emilia earthquake. *Soil Dynamics and Earthquake Engineering* 124: 389–398.

Conti, R., Angelini, M. & Licata, V. 2020. Nonlinearity and strength in 1D site response analyses: A simple constitutive approach. *Bulletin of Earthquake Engineering* 18: 4629–4657.

Cubrinovski, M., Bray, J.D., Taylor, M., Giorgini, S., Bradley, B. A., Wotherspoon, L. & Zupan, J. 2011. Soil liquefaction effects in the central business district during the February 2011 Christchurch earthquake. *Seismological Research Letters* 82: 893–904.

Hancock, J. & Bommer, J. J. 2005. The effective number of cycles of earthquake ground motion. *Earthquake Engineering & Structural Dynamics* 34(6): 637–664.

Hardin B.O. & Drnevich VP 1972. Shear modulus and damping in soils: design equations and curves. *Journal of the Soil mechanics and Foundations Division* 98(7): 667–692.

Idriss, I.M. & Boulanger, R.W. 2006. Semi-empirical procedures for evaluating liquefaction potential during earthquakes. *Soil Dynamics and Earthquake Engineering* 26(2–4): 115–130.

Idriss, I.M. & Boulanger, R.W. 2008. *Soil liquefaction during earthquakes*. Earthquake Engineering Research Institute.

Kramer, S.L. 1996. *Geotechnical earthquake engineering*. Pearson Education India.

MATLAB. 2021. *version 9.10.0 (R2021a)*. Natick, Massachusetts: The MathWorks Inc.

Miner, M.A. 1945. *Cumulative damage in fatigue*. Trans. ASME 67, A159–A164.

Mucciarelli, M. & Liberatore, D. 2014. Guest editorial: the Emilia 2012 earthquakes, Italy. *Bulletin of Earthquake Engineering* 12: 2111–2116. https ://doi.org/10.1007/s1051 8-014-9629-6

Phillips, C. & Hashash, Y. M. 2009. Damping formulation for nonlinear 1D site response analyses. *Soil Dynamics and Earthquake Engineering* 29(7): 1143–1158.

Seed, H.B. & Booker, J.R. 1977. Stabilization of potentially liquefiable sand deposits using gravel drains. *Journal of Geotechnical Engineering Division* 103(7): 757–768.

Seed, H.B., Martin, P.P., & Lysmer, J. 1975. *The generation and dissipation of pore water pressures during soil liquefaction*. College of Engineering, University of California.

Sorrentino, L., Liberatore, L., Decanini, L.D., Liberatore, D. 2013a. The performance of churches in the 2012 Emilia earthquakes. *Bulletin of Earthquake Engineering* 12: 2299–2331. doi:10.1007/s10518-013-9519-3

Sorrentino, L., Liberatore, L., Liberatore, D., Masiani, R. 2013b. The behaviour of vernacular buildings in the 2012 Emilia earthquakes. *Bulletin of Earthquake Engineering* 12: 2367–2382. doi:10.1007/s10518-013-9455-2

Terzaghi, K. (1923). Die Berechnung der Durchassigkeitsziffer des Tones aus dem Verlauf der hydrodynamischen Spannungs. erscheinungen. Sitzungsber. Akad. Wiss. Math. Naturwiss. Kl. Abt. 2A 132: 105–124

Tonni, L., et al. 2015. Analisi dei fenomeni deformativi indotti dalla sequenza sismica emiliana del 2012 su un tratto di argine del Canale Diversivo di Burana (FE). *Rivista Italiana di Geotecnica* 49(2): 28–58. [in Italian]

Trifunac, M.D. & Brady A.G. 1975. A study on the duration of strong earthquake ground motion. *Bulletin of the Seismological Society of America* 65(3): 581–626.

Tropeano, G., Chiaradonna, A., d'Onofrio, A. & Silvestri, F. 2016. An innovative computer code for 1D seismic response analysis including shear strength of soils. *Géotechnique* 66(2), 95–105.

Viggiani, G.M.B. & Atkinson, J.H. 1995. Stiffness of fine-grained soil at very small strains. *Géotechnique* 45(2): 249–265.

Wichtmann, T. & Triantafyllidis, T. 2009. Influence of the grain-size distribution curve of quartz sand on the small strain shear modulus Gmax. *Journal of Geotechnical and Geoenvironmental Engineering*, ASCE 135(10): 1404–1418.